

Influence of Thermal Disorders on XAFS Debye-Waller Factor of Nickel

Le Quang Thanh¹, Nguyen Thi Minh Thuy^{*2}

^{1,2}Faculty of Fundamental Sciences, University of Fire Prevention and Fighting, Hanoi 120602, Vietnam

ABSTRACT: The anharmonic X-ray absorption fine structure Debye-Waller factor of Nickel has been analyzed under the influence of thermal disorders. This Debye-Waller factor was calculated in explicit forms using the anharmonic correlated Debye model that developed from the correlated Debye model based on an anharmonic effective potential and the many-body perturbation approach. The thermodynamic parameters are derived from the influences on the absorbing and backscattering atoms caused by all their nearest neighbors in the crystal lattice with thermal vibrations. The numerical results of the Nickel in the temperature range from 0 to 800 K agree well with those obtained by the other theoretical models and experiments.

KEYWORDS: XAFS Debye-Waller factor; thermal disorders; metallic Nickel; Debye model.

I. INTRODUCTION

In recent years, the X-ray absorption fine structure (XAFS) has been widely used to determine many thermodynamic properties and structural parameters of materials, so it has been developed into a powerful technique [1]. However, thermal vibration disorders lead to the anharmonic effect of XAFS oscillation and will smear out the XAFS signals [2], as seen in Figure 1.

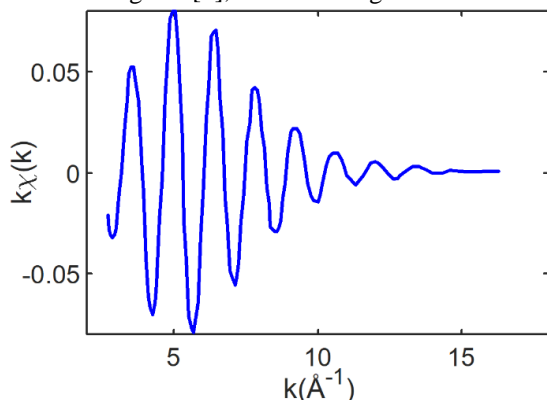


Figure 1. The XAFS signal $k\chi(k)$ of Ni at 300 K obtained from the experimental data [3].

In the investigation of the anharmonic XAFS signal, the anharmonic XAFS Debye-Waller (DW) factor $W(T, k)$ [4] is an important parameter because it can describe the anharmonic XAFS amplitude reduction. It is usually defined in the following form [5]:

$$W(T, k) = \exp\{-2k^2\sigma^2\},$$

(1)

where σ^2 is the mean-square relative displacement

(MSRD) and is the second XAFS cumulant.

Nowadays, Nickel (Ni) plays an important role in our daily lives, and Nickel-containing products possess better corrosion resistance, greater toughness, more strength at high and low temperatures, and a range of special magnetic and electronic properties [6]. Meanwhile, the experiment measured the second XAFS cumulants of Ni at the Synchrotron Radiation Siberian Center (SRSC), Russia, by Pirog *et al.* [3].

Recently, an anharmonic correlated Debye (ACD) model has been applied to effectively treat the anharmonic XAFS oscillation of metals [7]. The advantage of this model is that it can take into account the phonon-dispersion effect and acoustic phonon branch for crystals in both the low-temperature (L.T.T) and high-temperature (H.T.T) regions [8]. Still, it has not yet been used to analyze the anharmonic XAFS DW factor of Ni. Hence, the analysis and calculation of the anharmonic XAFS DW factor of Ni using the ACD model will be a necessary addition to experimental data analysis in the advanced XAFS technique.

II. FORMALISM AND CALCULATION MODEL

Usually, the Morse potential can validly determine the pair interaction (PI) potential of the crystals [9, 10]. If this potential is expanded up to the three orders around its minimum position, it can be written as

$$\varphi(x) = D(e^{-2\alpha x} - 2e^{-\alpha x}) \cong -D + D\alpha^2 x^2 - D\alpha^3 x^3 + \frac{7}{12} D\alpha^4 x^4, \quad x = r - r_0,$$

(2)

where D is the dissociation energy, α is the width of the potential, x is the deviation distance between the backscattering and absorbing atoms, and r and r_0 are the

instantaneous and equilibrium bond length between atoms, respectively.

To determine the thermodynamic parameters of a system, it is necessary to specify its anharmonic effective (AE) potential and force constants [11]. The AE potential in the relative vibrations of backscattering (A) and absorbing (B) atoms [12] can be calculated from the PI potential:

$$V_{eff} = V(x) + \sum_{i=A,B} \sum_{j \neq A,B} V(\varepsilon_i x \hat{R}_{AB} \hat{R}_{ij}), \quad \varepsilon_i = \frac{\mu}{M_i}, \quad (3)$$

where $\mu = M_A M_B / (M_A + M_B)$ is the reduced mass of the backscatter with masse M_A and absorber with masse M_B , sum i is the over backscatter ($i = A$) and absorber ($i = B$), the sum j is over the nearest neighbors, \hat{R} is a unit vector, $V(x)$ is a PI potential of these atoms, $V(\varepsilon_i x \hat{R}_{AB} \hat{R}_{ij})$ express the contribution of nearest-neighbor atoms to $V(x)$.

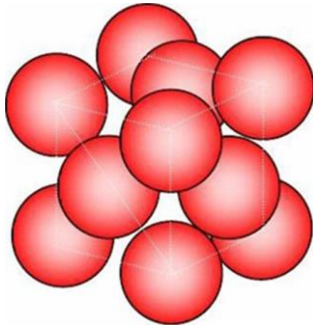


Figure 2. The structural model of Ni.

The structural model of Ni is illustrated in Figure 2. This structure has similar atoms at one center and eight corners of a cube [13], so each atom has a mass of m , and each unit cell contains two atoms [14]. After using structural characteristics, the AE potential of Ni is calculated from Eq. (3) and is written as

$$V_{eff}(x) = \varphi(x) + 4\varphi(0) + 2\varphi\left(-\frac{x}{2}\right) + 8\varphi\left(\frac{x}{4}\right) + 8\varphi\left(-\frac{x}{4}\right), \quad (4)$$

The result of A.E.E potential can be obtained from Eq. (4) using Morse potential in Eq. (2). If ignoring the overall constant, it is presented in the form:

$$V_{eff}(x) = \frac{1}{2} k_{eff} x^2 - k_{an3} x^3 + k_{an4} x^3, \quad (5)$$

where k_{eff} is the effective force constant, and k_{an3} and k_{an4} is an anharmonic force constants [11], which are not the temperature-dependent and are written as

$$k_{eff} = 5D\alpha^2, \quad k_{an3} = \frac{5}{4} D\alpha^3, \quad k_{an4} = \frac{133}{192} D\alpha^4, \quad (6)$$

The ACD model is derived from the dualism of an elementary particle in quantum theory and is perfected based on the correlated Debye model using the AE potential and many-body perturbation approach [7]. In this model, each atomic thermal vibration in the crystal lattice can be quantized and treated as a phonon that has a frequency $\omega(q)$ and is described via the dispersion relation. And these vibrations can be characterized by the correlated Einstein temperature θ_D and frequency ω_D [8]. These parameters can be defined as follows:

$$\omega_D = 2\sqrt{\frac{k_{eff}}{m}} = 2\alpha\sqrt{\frac{5D}{m}}, \quad \theta_E = \frac{\hbar\omega_E}{k_B} = \frac{2\hbar\alpha}{k_B} \sqrt{\frac{5D}{m}}, \quad (7)$$

$$\omega(q) = \omega_D \left| \sin\left(\frac{qa}{2}\right) \right|, \quad |q| \leq \frac{\pi}{a}, \quad (8)$$

where q is the phonon wavenumber in the first Brillouin (FB) zone, a is the lattice constant, and \hbar and k_B are the reduced Planck and Boltzmann constants, respectively.

Usually, the second XAFS cumulant can be presented in terms of the power moments of the real radial pair distribution (RPD) function [15]. The general expressions of the temperature-dependent XAFS cumulants in the ACD model were calculated by Hung *et al.* [7]. Substituting the expressions of local force constants k_{eff} and k_{an} in Eq. (6) into this general expression, and after converting from variable q to variable p in the formula $p = qa/2$, we obtain the temperature-dependent second XAFS cumulant in the form as

$$\sigma^2(T) = \langle x^2 \rangle - \langle x \rangle^2 = \frac{\hbar}{5\pi D\alpha} \int_0^{\pi/2} \omega(p) \frac{1 + \exp\{-\hbar\omega(p)/k_B T\}}{1 - \exp\{-\hbar\omega(p)/k_B T\}} dp, \quad (9)$$

Substituting this cumulant into Eq. (1) to calculate the temperature-dependent XAFS DW factor of Ni, we obtain the following result:

$$W(T, k) = \exp\left\{ -\frac{2\hbar k^2}{5\pi D\alpha} \int_0^{\pi/2} \omega(p) \frac{1 + \exp\{-\hbar\omega(p)/k_B T\}}{1 - \exp\{-\hbar\omega(p)/k_B T\}} dp \right\}, \quad (10)$$

Using the approximations $\exp\{-\hbar\omega(p)/k_B T\} \approx 0$, we calculate the XAFS DW

factor of Ni in the L.T.T limit ($T \rightarrow 0$) from Eq. (10). The obtained result is

$$W(k, T) = \exp\left\{-\frac{4\hbar k^2}{\sqrt{5\pi\alpha}\sqrt{Dm}}\right\},$$

(11)

Using the approximation $\exp\{-\hbar\omega(p)/k_B T\} \approx 1 - \hbar\omega(p)/k_B T$, we calculate the XAFS DW factor of Ni in the high-temperature (H.T.T) limit ($T \rightarrow +\infty$) from Eq. (10). The obtained result is

$$W(T, k) = \exp\left\{-\frac{2k_B k^2 T}{5D\alpha^2}\right\},$$

(12)

Thus, the ACD model has been extended to efficiently calculate the XAFS DF factor of Ni in the temperature-dependent. The obtained temperature-dependent expressions using this model can satisfy all their fundamental properties.

III. RESULTS AND DISCUSSION

In this section, we use the atomic mass $m = 58.6934$ u [16] and Morse potential parameters $D = 0.4205$ eV and $\alpha = 1.4199$ Å⁻¹, and $r_0 = 2.780$ Å [9] in calculations. Using Eqs. (6) and (7), we calculate and obtain the local force constants $k_{eff} \square 4.2$ eVÅ⁻², $k_{an3} \square 1.5$ eVÅ⁻³, $k_{an4} \square 1.2$ eVÅ⁻⁴, the correlated Debye temperature $\theta_D \square 284.3$ K, and the correlated Debye frequency $\omega_D \square 3.7 \times 10^{13}$ Hz. Meanwhile, the obtained values from the experiment are $k_{eff} \square 3.9 \pm 0.5$ eVÅ⁻², $k_{an3} \square 1.6 \pm 0.5$ eVÅ⁻³, $k_{an4} \square 1.7 \pm 0.9$ eVÅ⁻⁴, $\omega_D \square 3.6 \pm 0.2 \times 10^{13}$ Hz, and $\theta_D \square 273.9 \pm 17.1$ K [3]. It can be seen that our results agree with the experimental values, especially for the correlated Debye temperature and frequency.

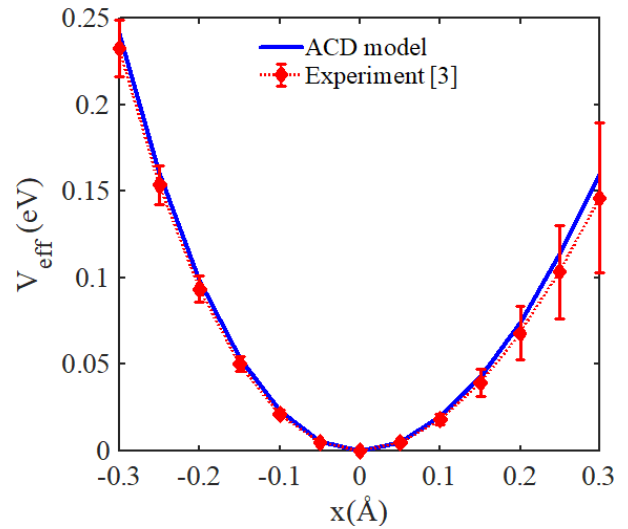


Figure 3. The position-dependent AE potential of Ni obtained from the ACD model and experiment.

The position dependence of the AE potential of Ni in the position range from -0.3 to 0.3Å is illustrated in Figure 3. Our obtained result using the ACD model is calculated using Eqs. (6) and (7), while the experimental result is obtained from Eq. (6) with the experimental values of local force constants [3]. It can be seen that our result agrees better with those obtained from the experimental data [3], especially near the equilibrium position ($x = 0$). Moreover, the further away from the equilibrium position, the anharmonic effect has a stronger influence on the AE potential, as seen in Figure 3. In addition, our obtained result using the ACD model is similar to those obtained with the quantum-correlated Einstein (QACE) [17] and classic-correlated Einstein (CACE) [18] models because all three models use the same AE potential.

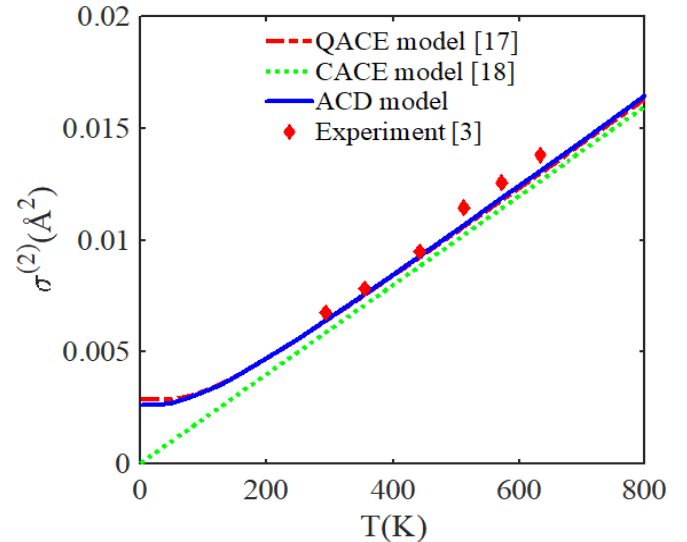


Figure 4. Temperature-dependent second cumulant of Ni obtained using the ACD, CACE, and QACE models and experiment.

The temperature dependence of the second XAFS cumulant $\sigma^2(T)$ of Ni in a range from 0 to 800 K is illustrated in Figure 4. Our obtained result using the ACD model is calculated by Eq. (9). It can be seen that our results are in agreement with those obtained using the QACE [17] and CACE (only at high temperatures) [18] models and experiment [3]. For example, the obtained results using the ACD model, QACE model, CACE model, and experiments at $T \approx 293$ K are $\sigma^2 \approx 6.4 \times 10^{-3} \text{ \AA}^2$, $\sigma^2 \approx 6.5 \times 10^{-3} \text{ \AA}^2$ [17], $\sigma^2 \approx 6.0 \times 10^{-3} \text{ \AA}^2$ [18], and $\sigma^2 \approx 6.8 \times 10^{-3} \text{ \AA}^2$ [3], respectively. Moreover, it can be seen that the ACD and QACE [17] models both show quantum effect contributions, but the obtained results using the QACE model [17] in the LT region are slightly greater. Meanwhile, the obtained result using the CACE model [18] reaches zero as the temperature reaches zero, so this model is unsuitable in the LT region. It is because this model only uses the classical statistical theory, so it cannot calculate quantum effects, as seen in Figure 4.

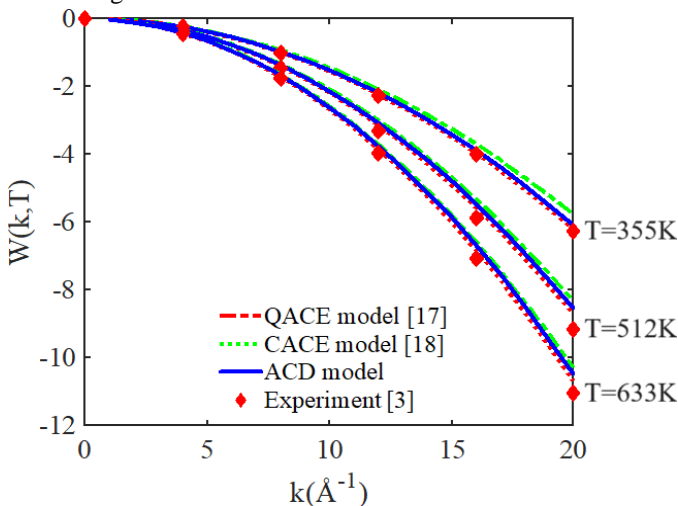


Figure 5. Wavenumber-dependent XAFS DW factor of Ni in the temperature change obtained using the ACD, QACE, and CACE models and experiment.

The wavenumber dependence of the anharmonic XAFS DW factor of Ni at 355 K, 512 K, and 633 K and in a range from 0 to 20 Å is illustrated in Figure 5. Herein, the obtained results using the QACE and CACE model are calculated by Eq. (1) with the temperature-dependent second XAFS cumulant determined in Refs. 17 and 18, respectively. The obtained results using the experiment are calculated by Eq. (1) with the experimental second XAFS cumulant [3], while our obtained results using the ACD model are calculated by Eq. (10). It can be seen that our results agree with those obtained using the QACE [17] and CACE [18] models and experiment [3], especially in comparison with the obtained results using the QACE model. For example, the obtained results using the ACD model, QACE model, CACE model, and experiments at

$T \approx 633$ K and $k = 15 \text{ \AA}^{-1}$ are $W \approx -6.6$, $W \approx -6.7$ [17], $W \approx -6.5$ [18], and $W \approx -7.1 \text{ \AA}^2$ [3], respectively. Moreover, the values of the XAFS DW factor decrease with fast-increasing wavenumber k and increasing temperature T . It is because the XAFS DW factor is an inverse function of the wavenumber k and second XAFS cumulant, in which this cumulant increases with increasing temperature T , as seen in Eq. (2) and Figure 4.

IV. CONCLUSION

In this work, we have expanded a calculation model to effectively analyze the anharmonic XAFS DW factor of Ni. The calculated expressions using the present ACD model satisfied all of their fundamental properties in the temperature-dependent. The anharmonic XAFS DW factor decreases with increasing temperature T , so the anharmonic XAFS amplitude decreases more intensely at higher temperatures. It is because the anharmonic XAFS amplitude is proportional to the anharmonic XAFS DW factor. This thermodynamic property shows that the higher the temperature, the stronger the X-ray absorption of the materials. These results can also describe the influence of anharmonic effects at high temperatures and the influence of quantum effects at low temperatures on the XAFS oscillation.

Our numerical results of Ni agree with those obtained using the QACE and CACE models and experiments at various temperatures. This agreement shows the effectiveness of the present model in investigating the anharmonic XAFS DW factor. This model can be applied to calculate and analyze the anharmonic XAFS DW factor of other metals from above 0 K to before the melting temperature.

ACKNOWLEDGMENTS

The author would like to thank Assoc. Prof. T.S. Tien for their helpful comments. This work was supported by the University of Fire Prevention and Fighting, Hanoi 120602, Vietnam.

REFERENCES

1. P. Fornasini, R. Grisenti, M. Dapiaggi, G. Agostini, and T. Miyanaga, Nearest-neighbour distribution of distances in crystals from extended X-ray absorption fine structure, *Journal of Chemical Physics* 147 (4) (2017) 044503.
2. P. Eisenberger and G. S. Brown, The study of disordered systems by EXAFS: Limitations, *Solid State Communications* 29 (6) (1979) 481-484.
3. I.V. Pirog, T.I. Nedoseikina, I.A. Zarubin, and A.T. Shuvaev, Anharmonic pair potential study in face-centered-cubic structure metals, *Journal of Physics: Condensed Matter* 14 (2022) 1825-1832.

4. R.B. Gregor and F.W. Lytle, Extended x-ray absorption fine structure determination of thermal disorder in Cu: Comparison of theory and experiment, *Physical Review B* 20 (12) (1979) 4902-4907.
5. N.V. Hung, C.S. Thang, N.B. Duc, D.Q. Vuong, and T.S. Tien, Temperature dependence of theoretical and experimental Debye-Waller factors, thermal expansion and XAFS of metallic Zinc, *Physica B: Condensed Matter* 521 (2017) 198-203.
6. J. Emsley, *Nature's Building Blocks: An A-Z Guide to the Elements*, 2nd edition, Oxford: Oxford University Press, 2011.
7. N.V. Hung, N.B. Trung, and B. Kirchner, Anharmonic Correlated Debye Model Debye-Waller Factors, *Physica B: Condensed Matter* 405 (11) (2010) 2519-2525.
8. T.S. Tien, L.D. Manh, N.T.M. Thuy, N.C. Toan, N.B. Trung, L.V. Hoang, Investigation of anharmonic EXAFS parameters of Ag using anharmonic correlated Debye model under the effect of thermal disorders, *Solid State Communications* 388 (2024) 115545.
9. L.A. Girifalco and V.G. Weizer, Application of the Morse Potential Function to Cubic Metals, *Physical Review* 114 (3) (1959) 687-690.
10. N.V. Hung, T.S. Tien, N.B. Duc, D.Q. Vuong, High-order expanded XAFS Debye-Waller factors of HCP crystals based on classical anharmonic correlated Einstein model, *Modern Physics Letters B* 28 (21) (2014) 1450174.
11. T. Yokoyama, K. Kobayashi, T. Ohta, and A. Ugawa, Anharmonic interatomic potentials of diatomic and linear triatomic molecules studied by extended x-ray-absorption fine structure, *Physical Review B* 53 (10) (1996) 6111-6122.
12. N.V. Hung and J.J. Rehr, Anharmonic Correlated Einstein-Model Debye-Waller Factors, *Physical Review B* 56 (1) (1997) 43-46.
13. S.H. Simon, *The Oxford Solid State Basics*, 1st edition, Oxford: Oxford University Press, 2013.
14. I.L. Shabalin, *Ultra-High Temperature Materials I*, New York: Springer, 2014.
15. L. Tröger, T. Yokoyama, D. Arvanitis, T. Lederer, M. Tischer, and K. Baberschke, Determination of Bond Lengths, Atomic Mean-Square Relative Displacements, and Local Thermal Expansion by Means of Soft-X-Ray Photoabsorption, *Physical Review B* 49 (2) (1994) 888-903.
16. N.W. Ashcroft and N.D. Mermin, *Solid State Physics*, 1st edition. New York: Holt-Rinehart & Winston, 1976.
17. T.S. Tien, Advances in studies of the temperature dependence of the EXAFS amplitude and phase of FCC crystals, *Journal of Physics D: Applied Physics* 53 (11) (2020) 315303.
18. T.S. Tien, Analysis of EXAFS oscillation of FCC crystals using classical anharmonic correlated Einstein model, *Radiation Physics and Chemistry* 186 (2021) 109504.